

## Stepwise Assembly of the Same Polyelectrolytes Using Host–Guest Interaction To Obtain Microcapsules with Multiresponsive Properties

Zhipeng Wang, Zhiqiang Feng, and Changyou Gao\*

Key Laboratory of Macromolecular Synthesis and Functionalization, Ministry of Education, and Department of Polymer Science and Engineering, Zhejiang University, Hangzhou 310027, China

Received February 1, 2008. Revised Manuscript Received April 3, 2008

Poly(allylamine hydrochloride) (PAH) derivatives, that is, PAH-g- $\beta$ -cyclodextrin (PAH-g- $\beta$ -CD) and PAH-g-ferrocene with the same positive charges on their chains, were synthesized and employed as building blocks to obtain multilayer microcapsules by using a host–guest interaction between the  $\beta$ -CD and ferrocene. Alternative assembly of PAH-g- $\beta$ -CD and PAH-g-ferrocene was conducted on sacrificial carbonate microparticles in a layer-by-layer (LbL) manner, followed by core dissolution with disodium ethylene diamine tetraacetate dihydrate (EDTA) to obtain the microcapsules. Step-wise increase of the layer thickness on silicone water was evidenced by ellipsometry, confirming the LbL growth mechanism. The hollow structure and morphology of the host–guest multilayer microcapsules were characterized by electron and scanning force microscopy. Owing to the charge interaction and host–guest interaction, the as-prepared microcapsules showed multiresponsiveness to pH, ionic strength, and host/guest molecules. For example, the capsule swelling and shrinking was observed at low and high pH and/or ionic strength, respectively. Progressive swelling of the microcapsules in  $\beta$ -CD solution was found also as a result of gradual decrease of the cross-linking degree contributed by the host–guest interaction. The capsule swelling and shrinking mediated by the change of pH and ionic strength is reversible at least for three cycles investigated so far. Using this feature, controllable loading and release of fluorescent probes was demonstrated.

### Introduction

Hollow microcapsules are of great interest because of their wide applications in fields of nanotechnology, biosensing and bioimaging, drug and gene delivery, and regenerative medicine.<sup>1–3</sup> So far various technologies have been developed to obtain the hollow capsules, among which the stepwise layer-by-layer (LbL) assembly has shown great success in fabricating microcapsules with layered structure and various functionalities.<sup>4–8</sup> The LbL technique, first introduced by Iler<sup>9</sup> and reestablished and refined by Decher,<sup>10</sup> assembles different building blocks onto sacrificial colloidal particles,

followed by core removal to produce the hollow capsules.<sup>11,12</sup> It shows great promise to precisely control the capsule structure and composition as well as to impart the capsule multifunction by incorporating various functional components.

It is known that a different driving force brings substantial differences of the microcapsules in terms of their chemical and physical structures, stability, and responsivity, and inevitably their functionality and applicability. However, the driving forces for the LbL assembly of microcapsules mainly began with the electrostatic attraction,<sup>13</sup> which limits the building blocks to a narrow range of oppositely charged and water soluble polymers. Recently, other driving forces such as hydrogen bonding and covalent bonding have been applied to obtain microcapsules with stimuli responsivity and ultra-stability, respectively.<sup>14–18</sup> For instance, by using the hy-

\* To whom correspondence should be addressed. E-mail: cygao@mail.hz.zj.cn.

- (1) Yang, L.; Alexandridis, P. *Curr. Opin. Colloid Interface Sci.* **2000**, *5*, 132.
- (2) Angelatos, A. S.; Katagiri, K.; Caruso, F. *Soft Matter* **2006**, *2*, 18.
- (3) Mal, N. K.; Fujiwara, M.; Tanaka, Y. *Nature* **2003**, *421*, 350.
- (4) Sukhorukov, G. B.; Antipov, A. A.; Voigt, A.; Donath, E.; Moehwald, H. *Macromol. Rapid Commun.* **2001**, *22*, 44.
- (5) Antipov, A. A.; Sukhorukov, G. B.; Moehwald, H. *Langmuir* **2003**, *19*, 2444.
- (6) Glinel, K.; Sukhorukov, G. B.; Moehwald, H.; Khrenov, V.; Tauer, K. *Macromol. Chem. Phys.* **2003**, *204*, 1784.
- (7) Radt, B.; Smith, T. A.; Caruso, F. *Adv. Mater.* **2004**, *16*, 2184.
- (8) Ma, Y. J.; Dong, W. F.; Hempenius, M. A.; Moehwald, H.; Vancso, G. J. *Nat. Mater.* **2006**, *5*, 724.
- (9) Iler, R. K. *J. Colloid Interface Sci.* **1966**, *21*, 569.
- (10) Decher, G. *Science* **1997**, *277*, 1232.

- (11) Donath, E.; Sukhorukov, G. B.; Caruso, F.; Davis, S. A.; Moehwald, H. *Angew. Chem., Int. Ed.* **1998**, *37*, 2201.
- (12) Caruso, F.; Caruso, R. A.; Moehwald, H. *Science* **1998**, *282*, 1111.
- (13) Sukhorukov, G. B.; Donath, E.; Davis, S.; Lichtenfeld, H.; Caruso, F.; Popov, V. I.; Moehwald, H. *Polym. Adv. Technol.* **1998**, *9*, 759.
- (14) Zhang, Y.; Guan, Y.; Yang, S.; Xu, J.; Han, C. C. *Adv. Mater.* **2003**, *15*, 832.
- (15) Kozlovskaya, V.; Ok, S.; Sousa, A.; Libera, M.; Sukhishvili, S. A. *Macromolecules* **2003**, *36*, 8590.
- (16) Zhang, Y.; Yang, S.; Guan, Y.; Cao, W.; Xu, J. *Macromolecules* **2003**, *36*, 4238.

drogen bonding between some uncharged polymers, Zhang et al.<sup>14</sup> have fabricated microcapsules with pH-sensitive properties. Akashi et al.<sup>17</sup> demonstrated that hollow microcapsules can be assembled from isotactic and syndiotactic poly(methyl methacrylate) stereocomplex by van der Waals interaction in a stepwise manner. We have recently used direct covalent assembly to fabricate microcapsules with ultrathin walls and high mechanical strength.<sup>18</sup>

Host–guest interaction is another type of driving force frequently employed in supramolecular chemistry. It combines H-bonding, hydrophobic force, and van der Waals force, which are usually formed between two determined molecules, typically exemplified by cyclodextrin (CD) and its guests.<sup>19–21</sup> For example, Reinhoudt<sup>22</sup> and co-workers reported that the self-assembled monolayer (SAM) containing  $\beta$ -cyclodextrin ( $\beta$ -CD) could be applied as “molecular printboards” to fix multivalent guest molecules. Liu et al.<sup>23</sup> showed that the inclusive complex of bifunctional  $\beta$ -CD and binaphthyl modified calix[4]arene could form a nanowire aggregate. Harada et al.<sup>24,25</sup> constructed a smart hydrogel by using  $\beta$ -CD and functional guest molecules of azobenzene and ferrocene, which can be mediated by the photo- and redox reactions. Although the great success and merits of the host–guest interaction have been shown in the area of supramolecular chemistry in terms of basic science,<sup>26,27</sup> very few attempts have been made to build LbL multilayer films using this interaction except in refs 28–30, let alone the multilayer microcapsules.

It is known that the host–guest interaction is readily mediated by the host and guest molecules with respect to their matching degree and concentration. For this context, host–guest multilayer microcapsules are fabricated by using an interaction between  $\beta$ -CD and ferrocene, known as a typical host–guest pair.<sup>31</sup> To exclude other driving forces such as charge attraction, the two molecules are grafted to the same polyelectrolyte, that is, poly(allylamine hydrochloride) (PAH). The other advantage of such a design is that multiresponsiveness of the microcapsules can be predicted, since the linkage between the  $\beta$ -CD/ferrocene inclusive is strong while the PAH chain is sensitive to pH and ionic

strength. Additionally, this design can eliminate the influence of other type of polymers in the shells,<sup>32–34</sup> and thus, it is easier to correlate the structure and properties of the microcapsules.

## Experiment Section

**Materials.** PAH ( $M_n = 70\,000$ ), TRITC–dextran (66 kDa), and FITC–dextran (19 kDa) were purchased from Aldrich.  $\beta$ -CD, *p*-toluenesulfonyl chloride, ferrocenecarboxaldehyde, NaBH<sub>4</sub>, EDTA, NaCl, and silicon wafers were commercial available products.  $\beta$ -CD and *p*-toluenesulfonyl chloride were purified by recrystallization in water and diethyl ether three times, respectively. Other chemicals were used as received. CaCO<sub>3</sub> particles with average diameters of 4, 5, and 10  $\mu\text{m}$  were prepared by rapidly mixing Ca(NO<sub>3</sub>)<sub>2</sub> solution and Na<sub>2</sub>CO<sub>3</sub> solution at different stirring rates and raw material concentrations.<sup>35</sup> The microparticles were collected by membrane filtration.

**Preparation and Characterization of Building Blocks and Host–Guest Microcapsules.** One of the primary hydroxyl groups of the  $\beta$ -CD was tosylated by *p*-toluenesulfonyl chloride, followed by substitution with an amino group of PAH (Mw 70 kD from Sigma-Aldrich) to obtain the PAH-g- $\beta$ -CD.<sup>36</sup> Ferrocenecarboxaldehyde was grafted to PAH, following by NaBH<sub>4</sub> reduction to obtain PAH-g-ferrocene.<sup>37</sup> Their chemical structures were confirmed by <sup>1</sup>H NMR spectra (Figure S1 in Supporting Information). The substituted degrees were found to be 14% for PAH-g- $\beta$ -CD and 15% for PAH-g-ferrocene by element analysis and atom absorption spectroscopy, respectively.

A suspension of spherical CaCO<sub>3</sub> particles (typically  $\varphi$  5  $\mu\text{m}$ , concentration ca. 5 wt %) was alternately incubated in PAH-g- $\beta$ -CD aqueous solution (1 mg/mL, pH 6) and PAH-g-ferrocene methanol solution (1 mg/mL, neutral pH) for 10 min, respectively. Three washings were applied after each adsorption to remove the excess building blocks. After three bilayers of PAH-g- $\beta$ -CD/PAH-g-ferrocene were deposited, the CaCO<sub>3</sub> cores were removed by 0.1 M disodium ethylene diamine tetraacetate dihydrate (EDTA) for 10 min. After extensive washing with fresh EDTA, the medium was displaced with water. Scanning electron microscope (SEM) images were taken on a SIRION-100 (RAITH) SEM. Transmission electron microscope (TEM) images were taken on TECNAL-10, Philips, and JEOL JEM-200CX TEM, Japan. Copper grids coated with cellulose acetate films were used to support the samples.

**LbL Assembly of the Host–Guest Multilayers on Silicone Wafer.** The  $\gamma$ -aminopropyl triethoxysilane (APS)-modified silicone wafer was first treated with a glutaraldehyde (GA) solution (2 wt %) for 30 min to obtain the GA-modified wafer. By a reaction between the aldehyde groups and the amino groups of PAH-g-ferrocene, a PAH-g-ferrocene layer was covalently immobilized onto the silicone wafer. The assembly was then carried out by alternate incubation of the silicone wafer in the PAH-g- $\beta$ -CD aqueous solution (1 mg/mL) and the PAH-g-ferrocene methanol solution (1 mg/mL) for 10 min, with sufficient washing in water and methanol at each interval under sonication, respectively. Multilayer thickness was measured by a spectroscopic ellipsometer (M-2000 from J. A. Woollam Co., Inc.). Data was obtained from three angles (65°, 70°, and 75°) from 600 nm to 1700 nm. Thickness

- (17) Kida, T.; Mouri, M.; Akashi, M. *Angew. Chem., Int. Ed.* **2006**, *45*, 7534.
- (18) Feng, Z.; Wang, Z.; Gao, C.; Shen, J. *Adv. Mater.* **2007**, *19*, 3687.
- (19) Lehn, J. M. *Angew. Chem., Int. Ed. Engl.* **1990**, *29*, 1304.
- (20) Lehn, J. M. *Science* **1993**, *260*, 1762.
- (21) Lehn, J. M. *Supramolecular Chemistry*; Concepts and Perspectives: VCH, Weinheim, 1995; Chapter 1.
- (22) Huskens, J.; Deij, M. A.; Reinhoudt, D. N. *Angew. Chem., Int. Ed.* **2002**, *41*, 4467.
- (23) Liu, Y.; Li, L.; Fan, Z.; Zhang, H.; Wu, X.; Guan, X.; Liu, S. *Nano Lett.* **2002**, *2*, 257.
- (24) Tomatsu, I.; Hashidzume, A.; Harada, A. *Macromolecules* **2005**, *38*, 5223.
- (25) Tomatsu, I.; Hashidzume, A.; Harada, A. *Macromol. Rapid Commun.* **2006**, *27*, 238.
- (26) Szejtli, J. *Chem. Rev.* **1998**, *98*, 1743.
- (27) Rekharsky, M. V.; Inoue, Y. *Chem. Rev.* **1998**, *98*, 1875.
- (28) Crespo-Biel, O.; Dordi, B.; Reinhoudt, D. N.; Huskens, J. *J. Am. Chem. Soc.* **2005**, *127*, 7594.
- (29) Van der Heyden, A.; Wilczewski, M.; Labbé, P.; Auzély, R. *Chem. Commun.* **2006**, 3220.
- (30) Suzuki, I.; Egawa, Y.; Mizukawa, Y.; Hoshi, T.; Anzai, J. *Chem. Commun.* **2002**, 164.
- (31) Szejtli, J.; Osa, T. In *Comprehensive Supramolecular Chemistry*; Atwood, J. L., Davies, J. E. D., MacNicol, D. D., Vögtle, F., Suslick, K. S., Eds.; Pergamon: Oxford, 1996; Vol. 3, Chapter 10.

- (32) Tong, W. J.; Gao, C. Y.; Moehwald, H. *Macromol. Rapid Commun.* **2006**, *27*, 2078.
- (33) Khopade, A. J.; Caruso, F. *Chem. Mater.* **2004**, *16*, 2107.
- (34) Zhang, Y.; Guan, Y.; Zhou, S. *Biomacromolecules* **2005**, *6*, 2365.
- (35) Zhukhorukov, G. B.; Volodkin, D. V.; Günther, A. M.; Petrov, A. I.; Shenoy, D. B.; Moehwald, H. *J. Mater. Chem.* **2004**, *14*, 2073.
- (36) Hollas, M.; Chung, M.; Adams, J. *J. Phys. Chem. B* **1998**, *102*, 2947.
- (37) Hodak, J.; Etchenique, R.; Calvo, E. *J. Langmuir* **1997**, *13*, 2708.

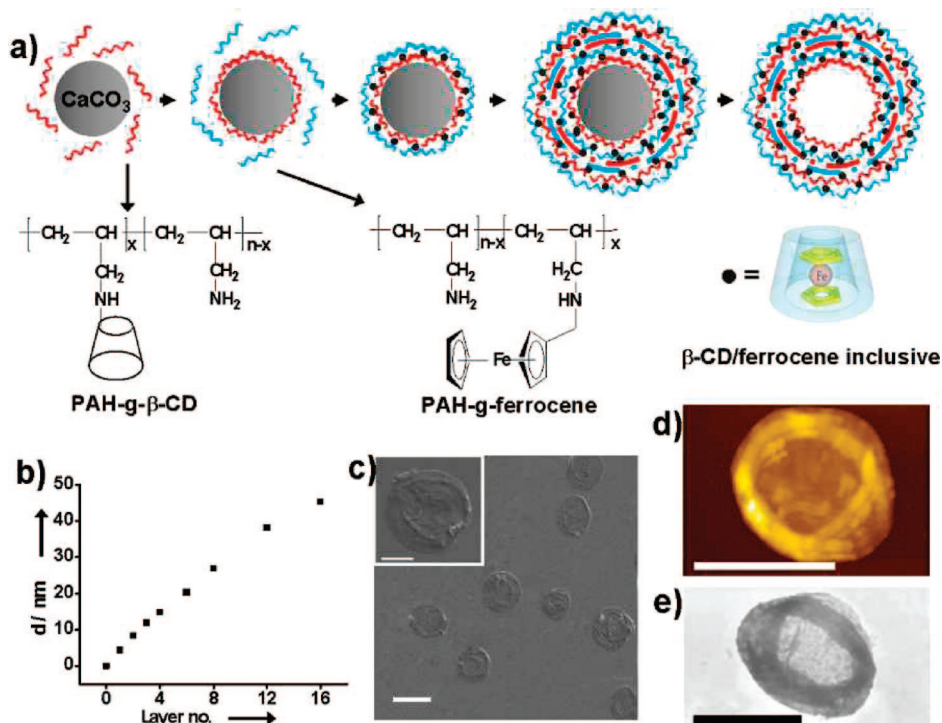


**Figure 1.** Fabrication process and structure characterization of host-guest microcapsules. (a) LbL assembly of the same polyelectrolyte on carbonate particles to obtain hollow microcapsules using host-guest interaction. The chemical structure of PAH-g- $\beta$ -CD, PAH-g-ferrocene, and  $\beta$ -CD/ferrocene inclusive are shown in the second row. (b) The thickness of the PAH-g- $\beta$ -CD/PAH-g-ferrocene multilayers assembled on silicone wafer as a function of layer number. (c) SEM, (d) SFM, and (e) TEM images of the prepared (PAH-g- $\beta$ -CD/PAH-g-ferrocene)<sub>3</sub> microcapsules, respectively; bar is 5  $\mu\text{m}$ . Inset in c is a higher magnification image of one capsule; bar is 2  $\mu\text{m}$ .

was obtained by fitting into Cauchy's model. Thickness of the covalently immobilized PAH-g-ferrocene layer was deduced from that of the whole multilayers, whose first layer was started from PAH-g- $\beta$ -CD.

**Microcapsules Swelling and Shrinking at Different Conditions.** The microcapsule size was averaged from all the capsules under a confocal laser scanning microscope (CLSM) image, which was obtained from a Zeiss LSM-510 or Bio-Rad Radiance 2100 CLSM after rhodamine 6G staining. At least 40 capsules were counted at each condition. In a typical experiment, the microcapsules were suspended in 20 mL of solution with a constant pH value (0.05 M phosphate at pH 6–9, HCl solution at pH 2–6, and NaOH solution at pH 9–13). Results showed that influence of the ionic strength (<0.05 M) on the capsule size is not significant compared with the pH value. Influences of ionic strength and  $\beta$ -CD concentration were similarly conducted.

For the scanning force microscope (SFM) experiment, a drop of the microcapsule suspension at a given pH value was applied onto a silicone wafer and dried immediately under a  $\text{N}_2$  flow to fix the capsules morphology. Topographical images of the microcapsules were obtained using a Seiko Instruments SPI3800N SFM with a dynamic force mode under ambient conditions.

## Results and Discussion

The stepwise assembly on  $\text{CaCO}_3$  particles with a diameter of 5  $\mu\text{m}$  was started from PAH-g- $\beta$ -CD, and then the PAH-g-ferrocene layer was assembled via the host-guest interaction as schematically shown in Figure 1a. Repeating for  $n$  cycles obtained core-shell particles, which gave (PAH-g- $\beta$ -CD/PAH-g-ferrocene) <sub>$n$</sub>  multilayer microcapsules after core removal (Figure 1c–e). The microcapsules were collapsed in a dry state to form the morphology of thicker periphery

and thinner center, confirming the hollow nature and continuous and intact shell structures. This type of morphology is rather typical for the microcapsules with relatively thicker shell thickness, 51 nm for the present ones, but is different from that of regular folds and creases of the traditional LbL polyelectrolyte microcapsules with thinner shell thickness, typically  $\sim 20\text{nm}$ . Of course the rigidity of the shells also should contribute to the capsule morphology, which needs further investigation. The SEM image (Figure 1c) reveals no apparent capsule coagulates and polymer aggregates on the capsule surface too. The same assembly was conducted on planar silicone wafer. Ellipsometry measurement (Figure 1b) revealed that thickness of the PAH-g- $\beta$ -CD/PAH-g-ferrocene multilayers was increased in a stepwise manner, confirming the LbL growth mechanism.

Since here the same PAH backbone was used for the assembly, the successful production of the hollow microcapsules can be only attributed to the host-guest interaction. To exclude other interactions unambiguously, control experiments were further conducted by substituting one of the PAH-g- $\beta$ -CD and PAH-g-ferrocene with PAH. The same assembly did not yield any capsules. The pair of PAH-g- $\beta$ -CD/PAH or PAH-g-ferrocene/PAH is dominated with charge repulsion, with absence of the attracting force. All the results confirm that the driving force for the capsule formation is definitely the host-guest interaction.

The host-guest interaction of CD and ferrocene is not influenced by the environmental pH and ionic strength, while the charge state of the PAH backbone is. By contrast, the host-guest interaction is sensitive to the treatment of host or guest molecules. Therefore, the as-prepared microcapsules



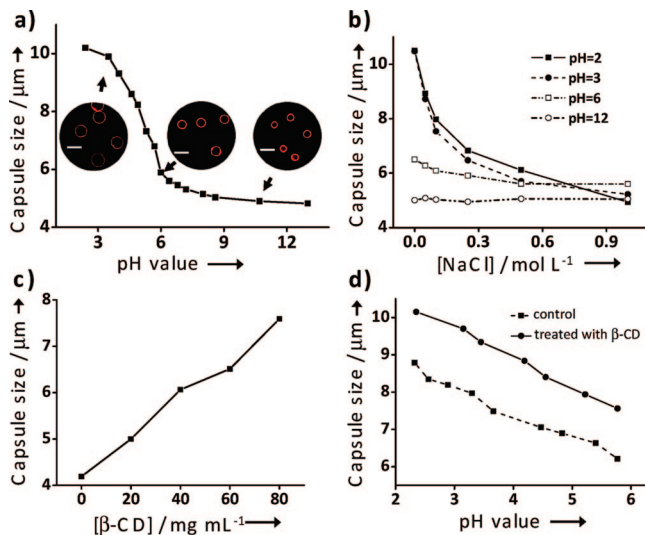


**Figure 2.** Swelling and shrinking of the host–guest microcapsules in response to various stimuli. The size of the host–guest microcapsules as a function of (a) pH value, (b) NaCl concentration, (c)  $\beta$ -CD concentration at 70 °C for 2 h, and (d) pH value after the microcapsules were incubated in 80 mg mL<sup>-1</sup>  $\beta$ -CD solution at 70 °C for 2 h. CaCO<sub>3</sub> particles with a size of 4  $\mu$ m were used here. Insets in (a) are CLSM images of the host–guest microcapsules at pH 3, 6, and 11 as indicated by the arrows.

with such a wall structure are expected to have multiresponsiveness. Systematic alteration of the capsule size as a function of the pH value is shown in Figure 2a. It reveals that the remarkable capsule swelling occurred progressively when the pH value was decreased, with a transition pH value of 5.2. For example (Figure 2a inset), at pH 6, the capsule size was 6  $\mu$ m. When the pH value was dropped to 3, the capsules were remarkably swollen to 10  $\mu$ m. The transition was rather sharp. By contrast, capsule shrinking at high pH was observed, but the extent was not obvious compared with their swelling. For example, at pH 11, the capsule size was found to be 5  $\mu$ m, which is equal to the core size exactly.

The pH triggered variation of the capsule size and morphology was further confirmed by SFM characterization, as representatively shown in Figure 3. Compared with the microcapsules dried at pH 6 (Figure 3b), those dried at pH 3 (Figure 3a) have a larger size and spreading pancake-like morphology with disappearance of the folds and creases, whereas those dried at pH 11 (Figure 3c) have a smaller size and more prominent folds and creases. The line profiles (Figure 3d) confirm the size variation and reveal further that the walls of the capsules (51 nm) became thinner (31 nm) and thicker (63 nm) when they were dried at acidic and alkaline conditions, respectively. Higher magnification of the flatter regions (insets of Figure 3a–c) confirms well the above conclusion and reveals that the average roughness within an area of  $1.2 \times 1.2 \mu\text{m}^2$  decreased from 7.8 nm (pH 6 dried) to 2.9 nm while they increased to 18.1 nm when they were dried at pH 3 and pH 11, respectively. Moreover, pore-like microstructure appeared on the pH 3 dried microcapsules (Figure 3a, inset).

The pH mediated capsule swelling and shrinking is understood as a result of alteration of the charge repulsion between the PAH backbone.<sup>38,39</sup> At an acidic condition the

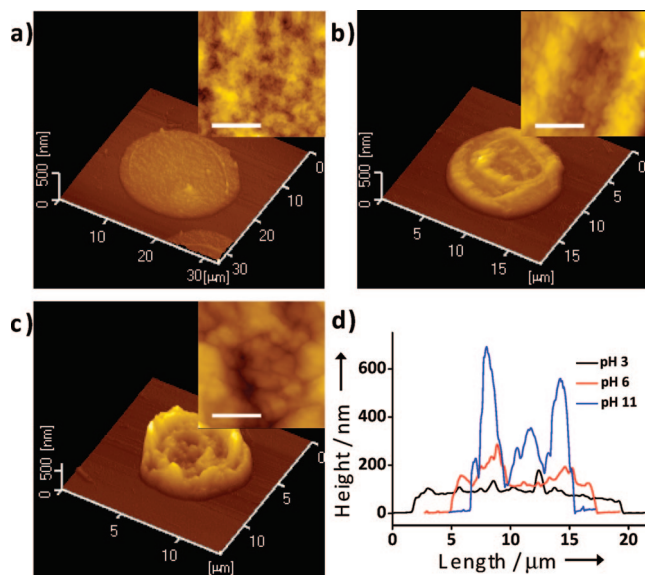


**Figure 3.** SFM images of the host–guest microcapsules dried at different pH values. The drying pH: (a) 3, (b) 6, and (c) 11. CaCO<sub>3</sub> particles with a size of 10  $\mu$ m were used here. Insets are higher magnification of a flat region on a microcapsule, respectively; bar is 500 nm. (d) Line profiles recorded from (a) to (c), respectively.

amino groups of PAH are highly protonated to create strong charge repulsion between the chains, leading to the capsule swelling. At an alkaline condition, by contrast, the charge is neutralized to lose the chain repulsion, leading to capsule shrinking.  $\zeta$ -potentials of the capsules ( $59.3 \pm 7.6$ ,  $18.0 \pm 6.3$  and  $5.5 \pm 2.6$  mV at pH 3, 6, and 11, respectively) are in good agreement with this explanation. Survival of the microcapsules at the extreme pHs reveals their strong ability to resist harsh conditions, raised exclusively from the host–guest interaction.

Now that the capsule swelling is caused by the charge interaction, the swelling degree can be then further modulated by ionic strength, which is an effective factor to screen the charge repulsion. At fixed pH values of 2, 3, 6, and 12, influence of NaCl concentration on the capsule size was explored. Figure 2b shows that along with increase of the NaCl concentration, the capsule sizes were decreased progressively, except at pH 12, in which the capsule size was not affected by the salt concentration. When the NaCl concentration reached 1 M, the capsule swelling at the acidic condition was completely inhibited regardless of the pH value of the investigated range. It has to be mentioned that a larger reduction degree was achieved by the same salt concentration if the original pH value of the capsule suspension was lower, indicating that the screening effect is more prominent in this case.

Apart from the pH and ionic strength, cross-linking degree of the capsule walls can be another factor to mediate the capsule swelling and shrinking. The multilayer walls of our microcapsules are held together by the  $\beta$ -CD/ferrocene inclusions between the PAH chains, that is, the cross-linking points. These cross-linking points can be destroyed by incubating the capsules in a solution of the host or guest molecules. In a typical experiment, the capsules were

(38) Hiller, J.; Rubner, M. F. *Macromolecules* **2003**, *36*, 4078.

(39) Kharlampieva, E.; Sukhishvili, S. A. *Langmuir* **2003**, *19*, 1235.

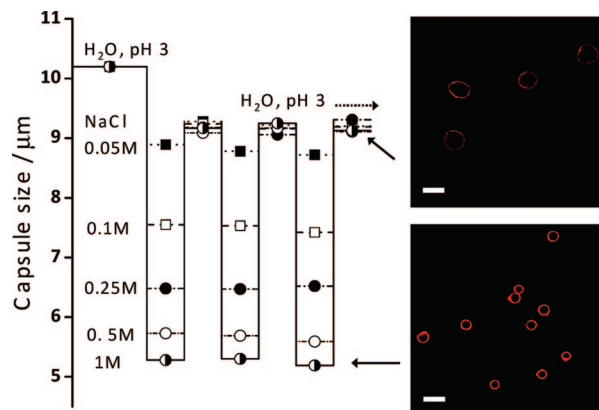


**Figure 4.** Reversible shrinking and swelling of the host–guest microcapsules. Three cycles of treatments in water and NaCl solution with a pH value of 3 are presented here. Typical CLSM images of the microcapsules after being treated for three cycles in water (upper) and in 1 M NaCl solution (lower), respectively; bar is 10  $\mu\text{m}$ .

incubated in a  $\beta$ -CD solution at pH 6 and 70  $^{\circ}\text{C}$  for 2 h ( $\beta$ -CD has poor solubility in water at room temperature; experimental results demonstrated that 2 h was long enough to reach an equilibrium state (Figure S2 in Supporting Information)). When the  $\beta$ -CD concentration was 0, the capsules experienced the same heat-induced shrinking as that of the LbL assembled polyelectrolyte capsules.<sup>40</sup> However, with increase of the  $\beta$ -CD concentration, the capsules expanded their sizes gradually (Figure 2c). In a free  $\beta$ -CD solution, the originally formed  $\beta$ -CD/ferrocene inclusions between the PAH chains will be partially substituted by the free  $\beta$ -CD/ferrocene inclusions. Consequently, the cross-linking degree of the capsule walls was decreased, leading to larger swelling of the capsules at the same pH value. In the next study, those microcapsules incubated in a free  $\beta$ -CD solution (80 mg/mL) at 70  $^{\circ}\text{C}$  for 2 h were subjected to acid treatment again, and their size variation was compared with the original ones (Figure 2d). Although the microcapsules showed a swelling behavior similar to that of the original ones along with the pH decrease, a larger swelling degree was recorded at each pH value. All these results illustrate that the host–guest microcapsules are readily multiple responsive, and their swelling and shrinking can be conveniently mediated by environmental stimuli such as pH, ionic strength, and  $\beta$ -CD concentration.

It has to be pointed out that the swelling and shrinking is mostly reversible supposing the stimuli are applied or eliminated. As shown in Figure 4, the microcapsules were swollen to  $>10 \mu\text{m}$  at pH 3, which shrunk for different extents upon incubation in NaCl solution depending on the salt concentration, for example, to  $\sim 5.3 \mu\text{m}$  in 1 M NaCl. Removal of the NaCl made the capsules recover their size to  $\sim 9.2 \mu\text{m}$ . For the next two cycles, swelling in pH 3 water and shrinking in the salt solution were completely reversible regardless of the salt concentration. Moreover, the microcapsules still maintained their spherical morphology and good dispersion as representatively shown in the insets of Figure

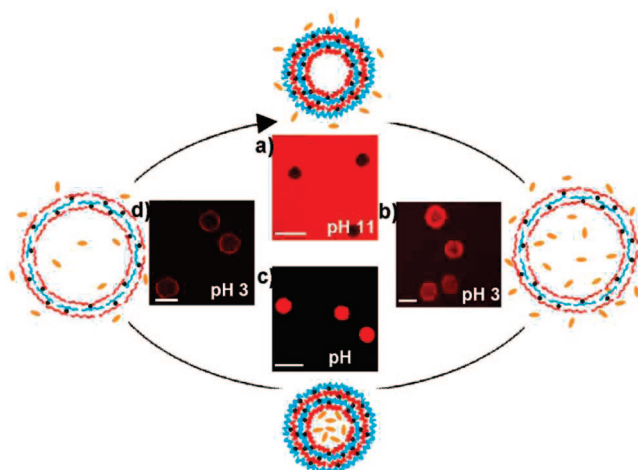


**Figure 5.** pH mediated loading and release of TRITC–dextran. At pH 11, the microcapsules shrank to retard the permeation of the TRITC–dextran (2 mg/mL) (a), whereas at pH 3, the microcapsules were swollen to permeate the free diffusion (b). After the microcapsules in (b) were quenched at pH 11, the probe was loaded (c), which was released again when the pH value was recovered to pH 3 (d). Bars in the CLSM images are 10  $\mu\text{m}$ . Within the cycle are CLSM images, and in the cycle are schematic cartoons of the capsule structures.

4. The non-recovered part equals  $\sim 10\%$ , which should be caused by the physical entanglement of chains during the first shrinking.

Utilizing the multiresponsiveness of the microcapsules, for example, swelling and shrinking, controllable loading and release of organic molecules and biomolecules such as enzymes, DNAs, biopolymers, and drugs can be conveniently realized. As a typical example, rhodamine labeled dextran (TRITC–dextran; 66 kDa) was loaded and released by the pH mediated swelling and shrinking of the capsules (Figure 5). At pH 11 the microcapsules were in a shrinking state and did not permit the TRITC–dextran molecules to penetrate into their interiors (Figure 5a). Hence, their interiors remained dark compared with the bulk solution. When the pH value was decreased to 3, capsule swelling occurred, causing the capsule wall to be in an open state (Figure 3a, inset) to permit diffusion of the TRITC–dextran molecules (Figure 5b). By quenching this capsule suspension in a pH 11 solution, the microcapsules shrank once again to entrap the TRITC–dextran molecules, as illustrated by the stronger emission from the capsule interiors (Figure 5c). Finally, the loaded TRITC–dextran could be released by incubating the microcapsules in pH 3 solution (Figure 5d). By the same procedure, FITC–dextran with a smaller Mw of 19 kDa was also loaded and released (Figure S3 in Supporting Information). The same concept was applied to the  $\beta$ -CD treated microcapsules, resulting in successful loading of FITC–dextran with a Mw of 250 kDa (Figure S4 in Supporting Information). It is worth mentioning that this loading and release is not restricted to the charge sign but controlled by permeation alteration of the capsule walls and, thus, is versatile to various molecules.

## Conclusion

The host–guest microcapsules that consist of PAH- $g$ - $\beta$ -CD and PAH- $g$ -ferrocene and show multiresponsiveness to

(40) Leporatti, S.; Gao, C.; Voigt, A.; Donath, E.; Moehwald, H. *Eur. Phys. J. E* **2001**, *5*, 13.

environmental stimuli have been successfully obtained in this study. By a strong host–guest interaction, the  $\beta$ -CD/ferrocene inclusives combine the repulsive PAH chains together so that the stepwise assembly of PAH-g- $\beta$ -CD/PAH-g-ferrocene can be achieved. Assembly of the PAH-g- $\beta$ -CD/PAH-g-ferrocene multilayers on carbonate cores followed by core removal produces the hollow capsules, whose good completeness and dispersivity are confirmed by SEM, TEM, SFM, and CLSM. The microcapsules show multiresponsiveness, for example, swelling and shrinking at low and high pH, respectively. Incubation in a salt or  $\beta$ -CD solution can also mediate their swelling and shrinking behavior. The swelling and shrinking is reversible for at least three cycles investigated so far. With these smart features, the microcapsules can function as reservoirs for drugs, DNA, enzymes, or other molecules, as exemplified here by loading and release of dextran. Therefore, this work not only enriches

the driving forces for fabricating the multilayer microcapsules but also produces multiresponsive microcapsules with a great potential for loading and release of desired substances in a precisely and conveniently controlled way.

**Acknowledgment.** We thank Prof. J.C. Shen for his continuous support and stimulating discussion. This study is financially supported by the Natural Science Foundation of China (No. 20434030, 20774084), the Major State Basic Research Program of China (No. 2005CB623902), and the National Science Fund for Distinguished Young Scholars of China (No.50425311).

**Supporting Information Available:** Additional figures including  $^1\text{H}$  NMR spectra, size of the host–guest microcapsules as a function of incubation time, pH mediated loading and release of FITC–dextran, and CLSM images (PDF). This material is available free of charge via the Internet at <http://pubs.acs.org>.

CM8003358